



Cervical vertebrae for early bone loss evaluation in osteoporosis mouse models

Bin Teng^{1#}, Xiang-Fang Yu^{1,2#}, Jian Li³, Anjaneyulu Udduttula⁴, Aynur Ismayil^{1,5}, Xinyue Huang¹, Junfeng Li^{1,2}, Pei-Yi Zhao^{1,2}, Goher Kerem^{1,5}, Jing Long³, Chang Liu^{1,2}, Pei-Gen Ren^{1,2}

¹Center for Energy Metabolism and Reproduction, Shenzhen Institutes of Advanced Technology, Chinese Academy of Sciences, Shenzhen, China; ²Shenzhen College of Advanced Technology, University of Chinese Academy of Sciences, Shenzhen, China; ³Center for Translational Medicine Research and Development, Institute of Biomedical and Health Engineering, Shenzhen Institutes of Advanced Technology, Chinese Academy of Sciences, Shenzhen, China; ⁴Centre for Biomaterials, Cellular and Molecular Theranostics, CBCMT, Vellore Institute of Technology, Vellore, India; ⁵Xinjiang Key Laboratory of Special Species Conservation and Regulatory Biology, College of Life Science, Xinjiang Normal University, Urumqi, China

Contributions: (I) Conception and design: B Teng, XF Yu, PG Ren; (II) Administrative support: X Huang; (III) Provision of study materials or patients: J Long; (IV) Collection and assembly of data: B Teng, XF Yu, A Udduttula, A Ismayil, J Li, PY Zhao, G Kerem, C Liu; (V) Data analysis and interpretation: B Teng, XF Yu, J Li; (VI) Manuscript writing: All authors; (VII) Final approval of manuscript: All authors.

[#]These authors contribute to this work equally.

Correspondence to: Pei-Gen Ren, PhD. Center for Energy Metabolism and Reproduction, Shenzhen Institutes of Advanced Technology, 1068 Xueyuan Avenue, Shenzhen University Town, Shenzhen 518055, China. Email: pg.ren@siat.ac.cn.

Background: Osteoporosis (OP), a systemic skeletal disease common in aged population, is an important public health problem worldwide. Animal models are important tools for understanding OP. In ovariectomy (OVX) or orchietomy (ORX) OP models, lumbar vertebrae are often used for evaluating of the OP progression. However, unlike the bipeds, the lumbar vertebrae are not weight loading bones in quadruped animal, but the head-bearing cervical vertebrae take much higher stress. So, we compared the murine cervical vertebrae with lumbar vertebrae for OP assessment.

Methods: OVX and ORX mouse models were established on C57BL/6J mice. Serum estradiol, testosterone and bone related biomarkers were verified. Bone quantity and quality were determined using micro computed tomography (micro-CT) analysis. Hard tissue sections were prepared, stained for histomorphological analyzing, and micro-indentation measured for bone mechanical property evaluation.

Results: In OVX and ORX mice, serum estradiol or testosterone levels reduced, bone resorption level and related biomarkers elevated, indicated the successful generation of the OP models. In the early stage, the trabecular bone mineral density (BMD) of cervical vertebrae was already reduced 16.1% (OVX) and 21.7% (ORX) one-month post-gonadectomy, respectively; while this decline in the fifth lumbar vertebra were only 5% and 7.4%, respectively. Six months post-gonadectomy, the reduction of BMD in cervical vertebrae and the fifth lumbar vertebra were 31.2% & 36.1% and 28.5% & 30.7% respectively. In biomechanical aspects, cervical spines showed worse Vickers hardness (HV) and elastic modulus than lumbar spine in six-month OVX and ORX mice.

Conclusions: We provide a new OP early-stage evaluation mouse model based on the cervical spine. Through the radiographic, biological and biomechanical assessments, the mouse cervical spine is more suitable for bone remodeling evaluation in OP models than the conventional lumbar vertebrae, especially for early-stage OP study.

Keywords: Murine osteoporosis model; cervical vertebrae; quadruped animal; biped animal; bone remodeling evaluation

Submitted Jul 06, 2022. Accepted for publication Feb 03, 2023. Published online Mar 20, 2023.

doi: 10.21037/qims-22-717

View this article at: <https://dx.doi.org/10.21037/qims-22-717>

Introduction

Osteoporosis (OP) is a well-known skeletal disease distinguished by the loss of bone mass and unusual alteration of bone micro-architectural structures, causing increased bone fragility and consequent bone fractures (1,2). This metabolic bone disorder is commonly occurred in both women and men. High rate bone mass reduction happens in elderly (3) and special population like astronauts (4). In current ageing decades, OP has become a major health problem due to its high morbidity, mortality, and significant health care cost. OP affects more than 200 million people globally (5). It was estimated that OP caused 1.3 million fractures (including about 500,000 vertebral, 250,000 hip, and 240,000 wrist fractures) and with annual expenditure over \$10 billion in United States in 2015 (6). In China, approximately 2.33 million osteoporotic fractures were occurred in 2010, costing \$9.45 billion. And, the number in China will reach 5.99 million fractures in 2050 (7). Clinically, the major types of human OP are post-menopausal, disuse, and glucocorticoid induced ones (8). Among them, the sex hormone deficiency (post-menopause or male androgen deficiency) related OP is the most common form.

OP causes systemic trabecular bone loss in vertebrae, hips, and wrists, predisposing these bone fractures (9). The incidences of fracture vary in different countries, but with an average rate up to 50% for women over 50 years old (2). Sex hormone deficiency related OP is also prevalent but often been underestimated in male aging population, and OP is one of the main causes of morbidity and mortality in this population (10,11). The Dubbo Osteoporosis study reveals that the 5-year post-fracture mortality and secondary fracture rate in men are higher than in their women counterpart (12).

To study and understand the pathogenesis and biological mechanisms of OP, a number of animal models have been developed (8,13,14). Among the models, mouse model is the most common used due to the feasibility of genetic modification, maturity, accessibility, and relatively low cost. The ovariectomy (OVX) and orchietomy (ORX) surgeries are most commonly used for generating sex-hormone deficiency murine models to imitate the human type I osteoporotic phenotype (8,13,15). Distal femur,

lumbar vertebrae, and proximal tibia are the major sites for evaluating the stage of OP in the mouse models (16). However, the quadrupedal rodent model is not a very suitable mimic from clinical perspective (14,17). There are big difference in anatomical and mechanical structures of the skeletal between bipeds (e.g., humans) and quadrupeds (rodents) due to their different natural body posture (18). The lumbar vertebrae of quadrupedalism rodents are sustained much less mechanical stress than which of bipedalism human; instead, the cervical vertebrae, which is responsible for supporting the head [which constitutes about 14% and 8% for the mouse (Figure S1) and rabbit body, respectively (19)], bears a greater mechanical burden. Therefore, we suggest that loading bear cervical vertebrae may be more suitable site for monitoring OP with femur to improve the efficiency and accuracy in mice model, rather than lumbar spine.

In this study, we have compared serum markers, microstructure, and biomechanical properties of cervical, lumbar vertebrae and femurs in OP and normal mice. The results show that the mouse cervical vertebrae present much earlier osteoporotic signs than lumbar vertebrae. In studies of musculoskeletal diseases like OP, the cervical spine can be a better detection site than the commonly used lumbar spine at early OP stage, and can be an alternative to save femoral tissues for those important biological evaluations. We present the following article in accordance with the ARRIVE reporting checklist (available at <https://qims.amegroups.com/article/view/10.21037/qims-22-717/rc>).

Methods

OP animal models

Wild type and healthy female and male C57BL/6J mice (7 weeks old, n=20) were purchased from Guangdong Medical Laboratory Animal Center (Guangdong, China). Animal were housed in SPF condition with a room controlled for temperature (20–26 °C), humidity (40–70%), maximum caging density was five, and with lights on from 8:00 AM to 8:00 PM. Female mice were subdivided into the following two groups with simple randomization by flipped a coin (n=5 per group): (I) sham operated (FM-sham) control, in which the ovaries were exposed but not

removed; (II) OVX surgery. Male mice were also subdivided into the following two groups by simple randomization (n=5 per group): (I) M-sham control, in which the testicles were exposed but not removed; (II) ORX surgery at 8 weeks of age. For animal sample size calculation, we set the significance level at 5% and power of study at 80%. Then, we have obtained the standard deviations of bone volume decrease percentage from previous reports was 11%, and we suggest the effect size of bone volume decrease percentage in our animal model would be 20%. According to the formula of previous study, the animal number in each group should be 5 (20).

The surgery was performed with proper anaesthesia by using ketamine with mice average weight were 22.1 ± 0.9 g [100 mg/kg body weight, intraperitoneally (*i.p.*)]. After the onset of anaesthesia, placed mice under infrared lamp on the operating table in laboratory to prevent heat loss. For female mice, a 0.5 cm single incision in the lower back was made. After located and exposed the ovary, a single ligature was performed around the oviduct 0.5 cm from ovary, and remove ovary by gently severing the oviduct for OVX mice, while replaced ovaries back into the abdominal cavity for FM-sham mice. For male mice, a 0.5 cm single incision on the ventral side of the scrotum. After exposed testicle, a single ligature was performed around the blood vessels and remove testis by gently severing blood vessels for ORX mice, replaced testicle back into the abdominal cavity for M-sham mice. Repeat the procedure for the other ovary or testis for OVX or ORX and suture the skin incision. Keep under close observation for approximately 4 h until mice fully recover from anaesthesia and then mice sent back to home cage. All the procedures were under the supervision and approved by the Ethics Committee for Animal Research, Shenzhen Institutes of Advanced Technology, Chinese Academy of Sciences (No. SIAT-IACUU-201225-YYs-TB-A1640), in compliance with institutional guidelines for the care and use of animals. After the completion of the surgery process, all mice showed a fast-physical recovery without problems and were allowed *ad libitum* access to water and diets for 6 months.

Serum biochemical marker measurements

First month after the surgery, about 400 mL of blood were collected from the retro-orbital sinus of mice (n=5 per group, total animal number =20) under isoflurane anesthesia. All animals showed a fast recovery, except one M-sham and ORX mice which died immediately.

Serum was obtained from the blood by centrifugation at 1,000 rpm for 30 min at 4 °C and immediately stored at -80 °C. Serum measured using ELISAs were processed according to the manufacturer's guidelines and measured against an inter-assay standard curve. We have tested the serum estradiol and testosterone levels to characterize the animal model. Then, the measurement of biochemical markers of bone turnover in serum including propeptide of type I procollagen (PINP, CSB-E12775m, CUSABIO, China), osteocalcin (OCN, CSB-E06917m, CUSABIO, China) and type I collagen C-telopeptide (CTX, CSB-E12782m, CUSABIO, China) to evaluate the process of OP with group information were blinded to assessors.

Micro-CT scanning

First or sixth months after the surgery, micro-CT scanning was performed to evaluate the bone parameter at cervical vertebrae, lumbar vertebrae and distal femurs. Due to the unique anatomic features of atlas (C1) and axis (C2) and the proximity of atlas-axis complex to C3 (21), C4–C7 of cervical vertebrae were selected for subsequent analysis. The first month of micro-CT scanning (n=5 per group, total mice number =20) were performed *in vivo* from the head to the feet of the mice under anesthesia with isoflurane. The six-month scanning (n=5 in FM-sham and OVX groups, n=4 in M-sham and ORX groups, total animal number =18) were performed after mice were euthanized with CO₂ and dissected free of soft tissue. A high-resolution micro-CT (Skyscan 1176, Bruker, Belgium) with a spatial resolution of 9 μm was used to scan the bone at a source voltage of 60 kV, a source current of 416 μA, with 2 average frames at every 0.5° angle step. Image reconstruction was performed using NRecon software, while smoothing was set to 1, ring artifact reduction was set to 5% and 40% beam hardening correction was applied with sample name were blinded to operators. Reconstructed data were further analyzed by CT-Analyzer through controlling the minimum grey threshold value was 80 HU (Hounsfield unit) and the maximum was 255 HU. Morphometric analysis was conducted to determine three-dimensional (3D) bone structures *in vivo*. Bone mineral density (BMD), bone volume/tissue volume ratios (BV/TV), trabecular thickness (Tb.Th), trabecular number (Tb.N), trabecular pattern factor (Tb.Pf) and structure model index (SMI) were analyzed using CTAn software (SkyScan, Kontich, Belgium). 3D reconstructed micro-CT images of bone were generated using CTvol software with group information were blinded to analyzers.

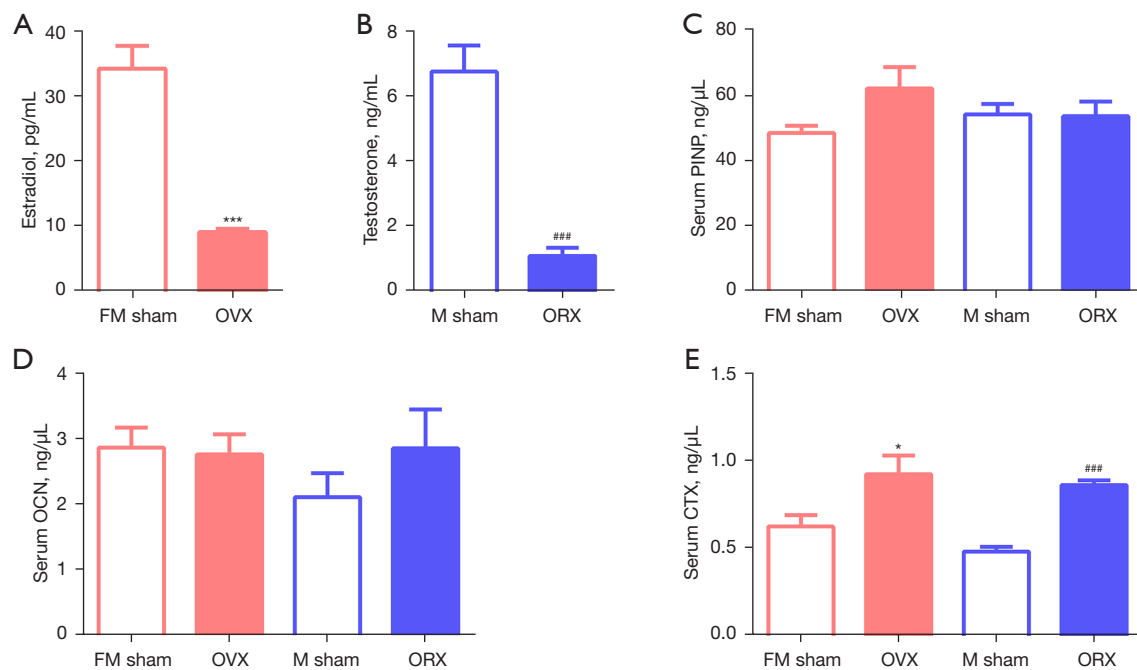


Figure 1 Serum bone turnover biomarkers in OVX, ORX and control groups one-month post-gonadectomy. (A) Estradiol level in the female sham and OVX group; (B) testosterone level in the male sham and ORX group; (C) PINP level; (D) OCN level; (E) CTX level. * $P < 0.05$, *** $P < 0.001$ when compare to sham group. ### $P < 0.001$ when compare to M-sham group. Five mice per group were analyzed. All data were presented as the mean \pm standard deviation. FM, female; OVX, ovariectomy; M, male; ORX, orchietomy; PINP, propeptide of type I procollagen; OCN, osteocalcin; CTX, C-terminal telopeptide.

Micro-indentation testing

The individual stained and dried specimen of each sample ($n=3$ per group, total animal number =12, see Appendix 1) with predefined region of interest (ROI) was subjected to micro-indentation using a Microhardness Tester (Future-Tech Corp., Tokyo, Japan) according to the procedure outlined by the International Organization for Standardization (ISO6507). Three ROIs in each slice were selected for micro-indentation testing. The Vickers diamond pyramidal indenter was compressed at 25 g compression load onto the ROI for a dwell time 10 s. An indentation mark formed on the ROI during the compression of the indenter, and the diagonal length of the indentation mark was then measured immediately under reflected light microscopy for the calculation of Vickers hardness (HV) and elastic modulus. The diagonal length of the indentation mark was measured immediately after the indentation to avoid the fast recovery of the indentation mark on the tissue matrix, especially for the soft tissues. For this reason, in order to obtain an average HV value, one sample should be made of three indentations. The average

HV of all nine ROIs in each group were calculated for statistical analysis with group information were blinded to analyzers.

Statistical analysis

No samples were excluded and all data were presented as the mean \pm standard deviation. All results were analyzed by one-way analysis of variance (ANOVA) followed with Tukey's multiple comparison test. The P values less than 0.05 were considered significant statistically.

Results

One-month post-gonadectomy, we didn't encounter any adverse events. In OVX mice, the serum estradiol was about 4-fold decreased; while in ORX mice, the serum testosterone was dropped nearly five times (Figure 1A,1B). Osteogenic markers PINP and OCN were not significantly affected in the models (Figure 1C,1D) (22), but the osteoclastic biomarker CTX (23) was significantly increased

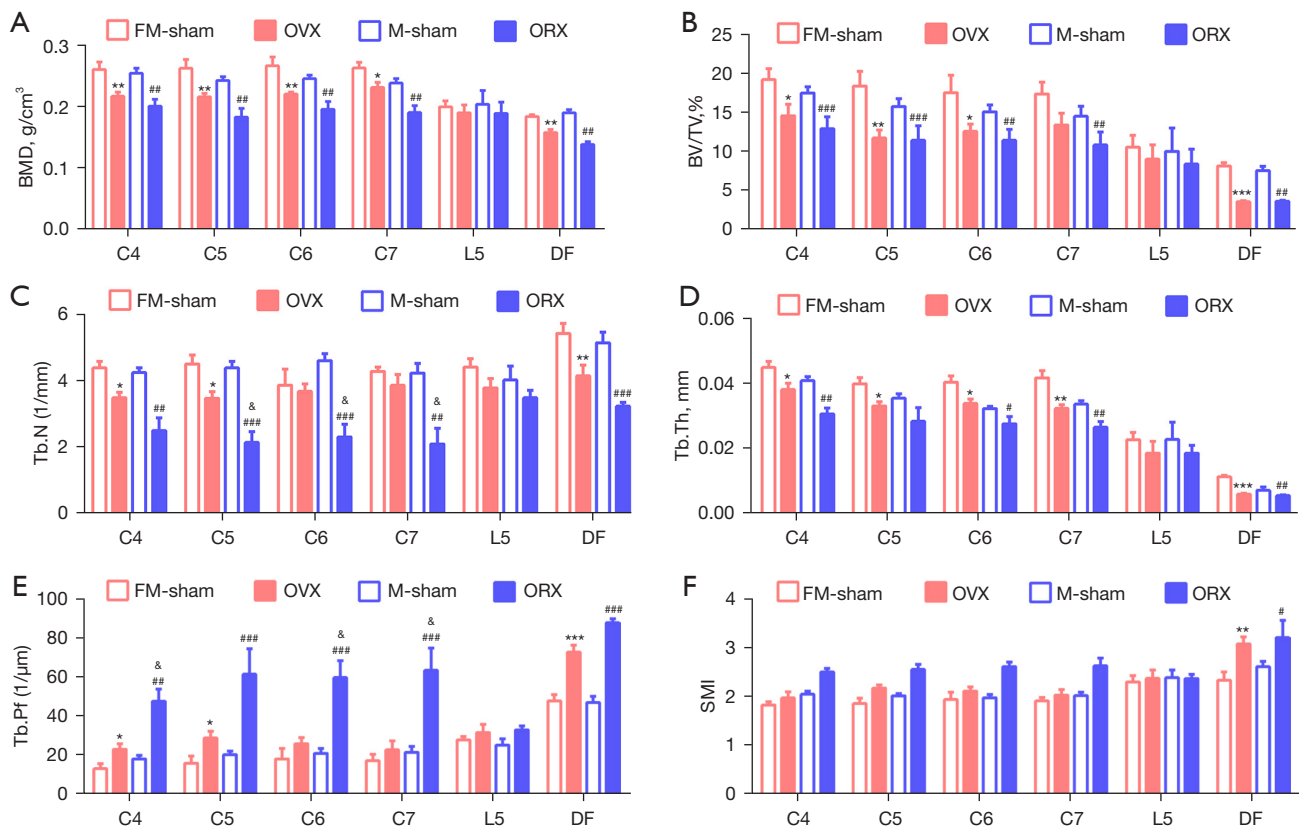


Figure 2 Cervical vertebra (C4–C7), lumbar vertebra (L5) and DF micro-CT scanning one-month post-gonadectomy. (A) BMD; (B) BV/TV; (C) Tb.N; (D) Tb.Th; (E) Tb.Pf; (F) SMI. * $P < 0.05$, ** $P < 0.01$, *** $P < 0.001$ when compare to FM-sham group. # $P < 0.05$, ## $P < 0.01$, ### $P < 0.001$ when compare to M-sham group. & $P < 0.05$ when compare to OVX mice group. Five mice per group were analyzed. All data were presented as the mean \pm standard deviation. BMD, bone mineral density; FM, female; OVX, ovariectomy; M, male; ORX, orchietomy; DF, distal femur; BV/TV, bone volume/tissue volume; Tb.N, trabecular number; Tb.Th, trabecular thickness; Tb.Pf, trabecular pattern factor; SMI, structure model index; CT, computed tomography.

in OVX or ORX mice (Figure 1E). MicroCT analysis of the animals also demonstrated the success of the OP model establishment (Figure 2).

One month after sex hormone deprived, the loss of bone mass was significantly higher in OVX and ORX groups than sham groups on cervicale and femur but not on fifth lumbar (Figure 2). The BMD of 4th, 5th, 6th and 7th cervical vertebrae BMD in OVX mice were significantly decreased (16.8%, 17.9%, 17.4% and 12.1%, respectively); ORX mice decreased significantly too, with an average 21.7% drop to the male sham mice. As the main load-bearing bone, femurs showed same trend as the cervicale, with the BMD dropped 14.3% and 27.3% in OVX and ORX mice, respectively. However, at this stage, the commonly used OP monitoring fifth lumbar vertebra presented obvious insensitivity to the sex-hormone deficiency, with only 5% ($P = 0.54$) and 7.4%

($P = 0.62$) non-significant decline in OVX and ORX groups, respectively (Figure 2A, Table 1).

As the BMD, other parameters including BV/TV, Tb.N and Tb.Th showed similar trends in cervical and lumbar vertebrae, and femurs (Figure 2B–2D). Moreover, we select the OP evaluating parameters Tb.Pf to show the trabecular connectivity and SMI to show the trabecular structure. The Tb.Pf was significantly increased in male cervical vertebrae, female cervical vertebrae (C4 and C5) and distal femur in the OVX or ORX mice, but not in the fifth lumbar spine (Figure 2E). Also, for SMI, cervical vertebrae showed the increase trend and the distal femur had significant increase, while the lumbar spine didn't change much (Figure 2F). Above results confirm that, in both female and male OP mice, the cervical vertebrae but not lumbar vertebra present OP characteristic at very early stage.

Table 1 Net decrease of OVX and ORX group mice compare to sham group in BMD

Site	Group	First month	Sixth month
C4	OVX	16.8%±6.2%***	29.7%±10.4%
	ORX	21.2%±8.9%###	34.8%±6.8%
C5	OVX	17.9%±6.2%***	32.3%±11.2%
	ORX	24.8%±11.8%###	40.3%±6.1%
C6	OVX	17.4%±3.4%***	31.4%±13%
	ORX	20.4%±10.5%###	34.4%±5.2%
C7	OVX	12.1%±8.6%***	31.7%±8.9%
	ORX	20.3%±9.4%###	34.7%±6.9%
CA	OVX	16%±6.5%***	31.3%±10.2%
	ORX	21.7%±9.3%###	36.1%±6.4%
L5	OVX	5.0%±6.9%	28.5%±15.2%
	ORX	7.4%±8.3%	30.2%±16.1%
Femur	OVX	14.3%±7.1%***	56.2%±2.5%***
	ORX	27.3%±5.1%###	69.1%±2.7%###

Data are presented as mean ± standard deviation. ***P<0.001 when compare to OVX lumbar data. ###P<0.001 when compare to ORX lumbar data. OVX, ovariectomy; ORX, orchietomy; BMD, bone mineral density; CA, cervical average.

Six-month post-gonadectomy, the OP reaches the late stage of OP with BMD reduced at least 30% (Figure 3A). The bone quantity and quality of OP mice was continuously deteriorated when compared to the early stage of OP (Figure 2, Figure S2). The average BMD and BV/TV of the cervical vertebrae were decreased 31.2% and 41.8% in OVX mice and 36.1% and 51.5% in ORX mice, respectively. Meanwhile, the lumbar spine also exhibited apparent significantly OP (Figure S2), with the average BMD and BV/TV decreased about 28.5% and 31.4% (OVX) and 30.2% and 45.7% (ORX), respectively, (Figure 3A, 3B, Table 1). The decrease trend of Tb.N and Tb.Th were paralleled with BV/TV, degree of the fifth lumbar spine descent is still less than the cervical spine (Figure 3C, 3D). Tb.Pf and SMI of cervical and lumbar spines was also showed a similar raising manner (Figure 3E, 3F). In addition, we have generated the 3D reconstructed micro-CT images for the cervical and lumbar spine in the first month (Figure S3) and sixth month (Figure 4). The images further confirmed that cervical and lumbar spine was both suffered severely bone mass loss in the late stage of the OP model.

In addition to micro-CT analysis, we have also performed histological and mechanical analysis to support our hypothesis (24). After hard-tissue section and staining, it was shown a significant bone area reduction in cervical and lumbar in the OVX and ORX groups (Figure S4). Based on the slices of hard-tissue section, the resistance of penetration was tested to reflect the hardness of cervical and lumbar vertebrae. In the previous studies, cancellous bone but not cortical bone is most affected after OVX in mice, we then selected the ROIs exclusive on the trabecular bone (Figure 5A) (25,26). The HV and elastic modulus were decreased both in cervical and lumbar vertebrae of OVX and ORX mice (Figure 5B, 5C). Meanwhile, the decline of HV in cervical vertebrae (36.3% and 33.3%) were significantly higher than lumbar vertebrae (26.2% and 24.3%) of OVX and ORX group (Figure 5D).

Discussion

OP and its associated fractures have become a major social health problem. Due to its “silent” characteristic, it is unaware until the fracture occurs (27). Hence, the monitoring of OP is very important in clinical practice and related animal model. Since 1960s, the high incidence of OP fracture bones like femur and lumbar vertebrae had become the major sites for OP monitoring (28,29). Since the poor correlation between different bones during OP (30), in clinical the T-score calculation usually involves lumbar spine, femur neck, or total hip for their BMD testing as the NIH suggested (30,31).

In quadruped experimental animals, however, the anatomical dimensions and mechanical properties were different from biped animals. Unlike human beings, the main force on the spine of animals is non compressive force (32,33). Measurements on sheep revealed that compressive forces of lumbar vertebrae were between 58 and 130 N, while which were 400–600 N in comparable body weight human beings (32). In another side, the head-carrying cervical spine was exposed to much higher stress (33). So, compare to usually used lumbar vertebrae BMD evaluation in experimental quadruped, we suggest that load-bearing cervical vertebrae could be a better site for monitoring OP with femur to improve the efficiency and accuracy. The data in present study manifest that microCT measurement of cervical vertebrae is a simple imaging method, with better OP evaluating value than lumbar spine, especially for the early-stage evaluation of OP.

In clinic of OP, women have received attention widely,

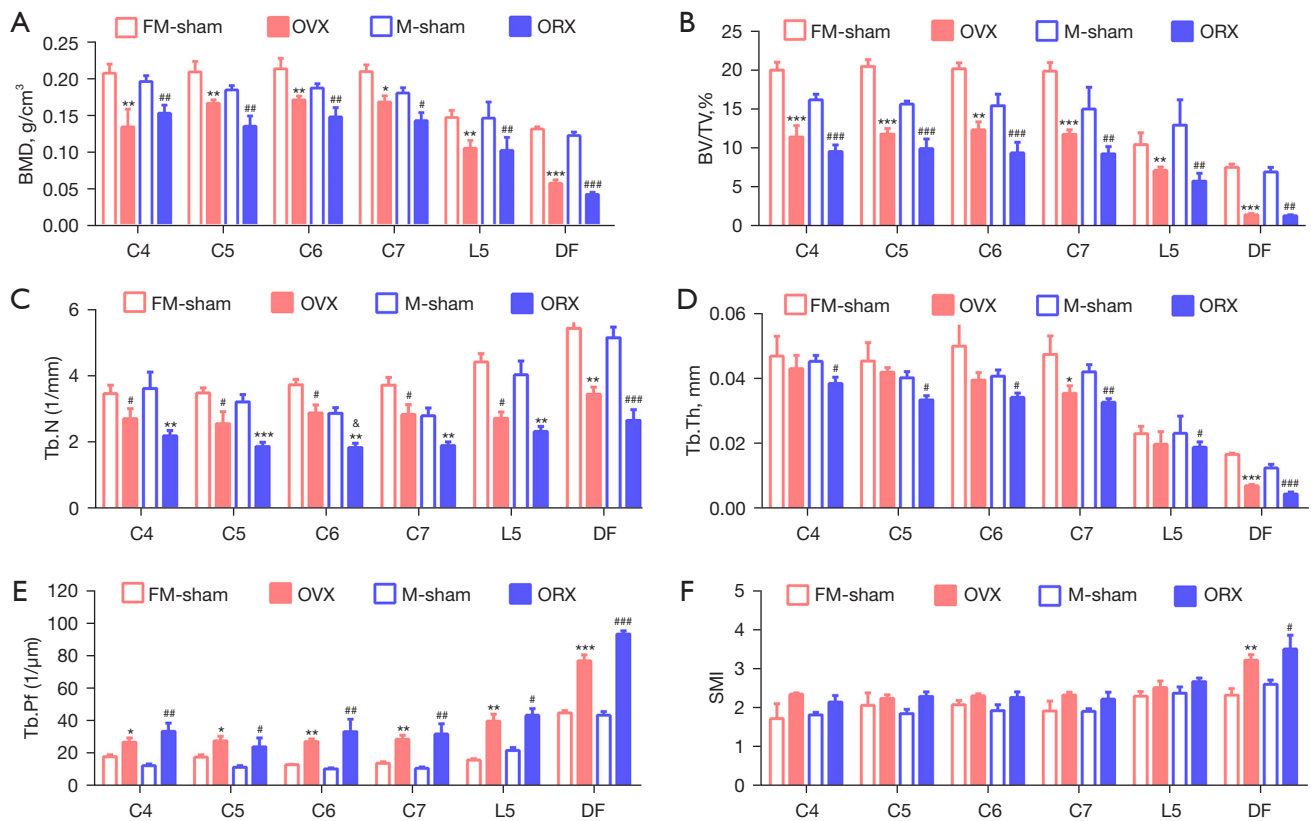


Figure 3 Cervical vertebra (C4–C7), lumbar vertebra (L5) and DF micro-CT scanning six-month post-gonadectomy. (A) BMD; (B) BV/TV; (C) Tb.N; (D) Tb.Th; (E) Tb.Pf; (F) SMI. * $P < 0.05$, ** $P < 0.01$, *** $P < 0.001$ when compare to FM-sham group. # $P < 0.05$, ## $P < 0.01$, ### $P < 0.001$ when compare to M-sham group. & $P < 0.05$ when compare to OVX mice group. Five mice in FM-sham and OVX groups. Four mice in M-sham and ORX groups were analyzed. All data were presented as the mean \pm standard deviation. BMD, bone mineral density; FM, female; OVX, ovariectomy; M, male; ORX, orchietomy; DF, distal femur; BV/TV, bone volume/tissue volume; Tb.N, trabecular number; Tb.Th, trabecular thickness; Tb.Pf, trabecular pattern factor; SMI, structure model index; CT, computed tomography.

while although androgen deficiency related OP is prevalent in male ageing population, it's often been underestimated (10,11,34). We included both female and male mice OVX and ORX models, try to get a portfolio of OP information of femur, cervical and lumbar vertebrae in both genders. In present study, the development of OP in the two animal models is generally similar, indicating that gender has less influence on it than we expected. Intriguingly, we found the ORX mice had surpassed OVX mice in the progress of OP in some aspects, such as such as Tb.N and Tb.Pf (Figure S3). Androgens, similar to estrogen, also have significant regulatory effects on the skeletal system (35). In clinic, OP has received more attention in women for the menopause. Meanwhile, androgen deficiency related OP is also prevalent but often been underestimated in male ageing population. Also, in the early stage of the model, the

residual level of estrogen is higher than that of androgen, this may influence the OP progression. Six months later, the disappearance of gender differences in Tb.Pf can also support the above suggestion.

Unsurprisingly, the OP of the mouse femurs occurred earlier and progressed most rapidly as described in the NIH guideline for human beings (31). However, which was not the same case for lumbar vertebrae, another suggested site in the guideline, showed a significant lag compare to both femur and cervical vertebrae in the first month. In both OVX and ORX mice, the trabecular parameters such as BMD, BV/TV, Tb.N and Tb.Th indicated that OP occurred in cervical spine, femur but not in lumbar spine at the first month. Half year later, all the 3 bone sites presented OP status. It's known that the progression of sex hormone deprived OP is a non-linear process, involved

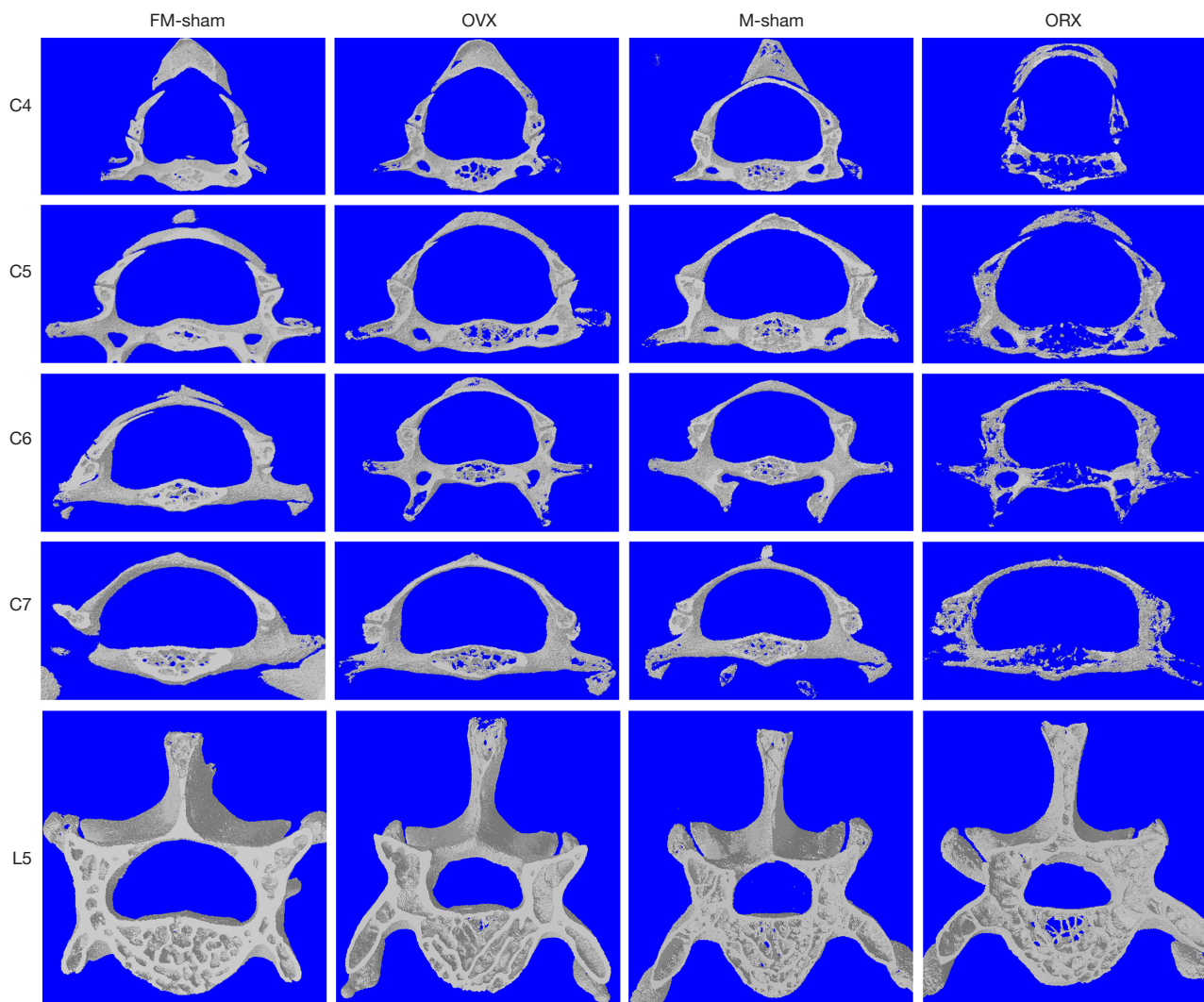


Figure 4 The exemplary 3D image from the micro-CT analysis of the different cervical vertebra and fifth lumbar from different group at 6th month. The female sham mice group, OVX mice group, male sham mice group and ORX mice group were shown from left to right in each column of the figure. FM, female; OVX, ovariectomy; M, male; ORX, orchietomy; CT, computed tomography.

rapid and gradual bone loss periods (36). The weight-loading bones in mice like femur and cervical spine could get into the rapid period much faster than the non-loading bone like lumbar spine. The sensitivity of cervical vertebra to OP supplies an early time window for OP monitoring, which is especially useful when the femur been occupied under surgeries or other treatments. In addition, we found that there's no statistic difference between the CA and the individual ones for the BMD (*Table 1*), which may suggest that we can scan and analyze C4-7 as a whole thing for OP evaluation.

We compared the OP indicator trabecular

microarchitecture parameters Tb.Pf and SMI in the animal models. Both Tb.Pf and SMI evaluate trabecular plate and rod patterns (37,38), in which plates considered to be superior to rods mechanically (39-41). However, it seems that Tb.Pf is not as 'stringent' as SMI for OP evaluation, for there's only femur tissue shown significant change for SMI while Tb.Pf presented more statistical significances in different bones at both time points. This could be explained algorithmically. The SMI evaluates the plate and rod pattern based only on the convex surface, however, the trabecular microstructure network also contains abundant concave surfaces (39). Also, unlike the long

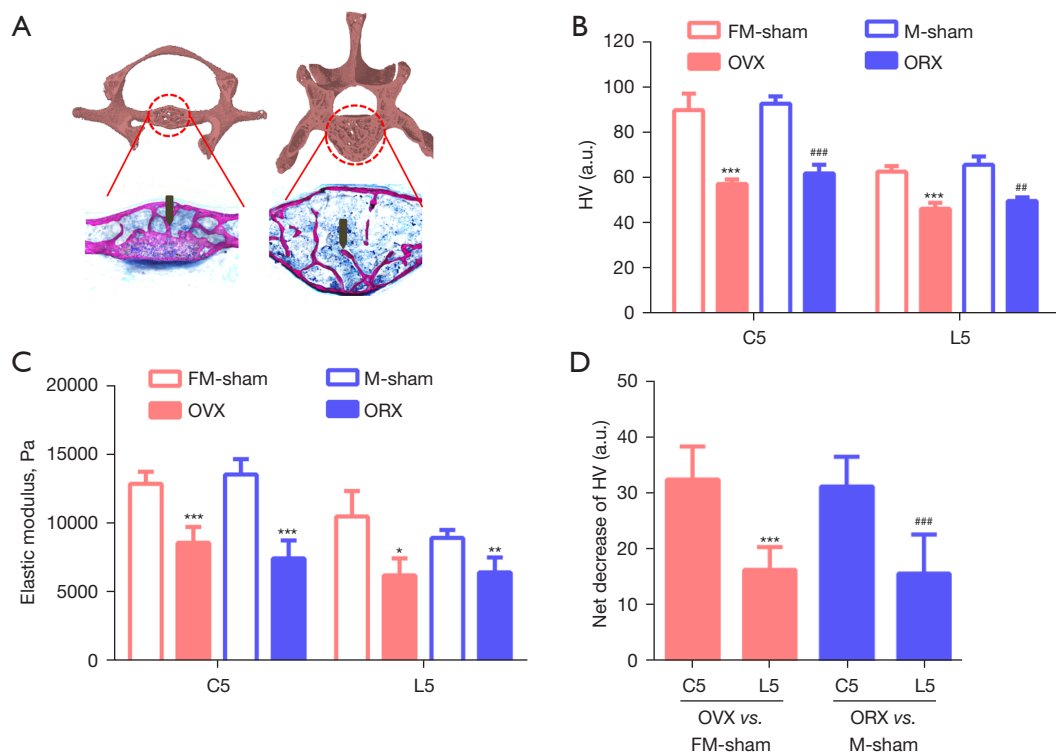


Figure 5 The cervical spine groups showed a more severe bone loss in OVX and ORX mice by mechanical analysis. (A) Diagram of micro indentation experiment; (B) Vickers hardness of cervical vertebra and fifth lumbar spine; (C) elastic modulus of cervical vertebra and fifth lumbar spine; (D) net decrease of the HV of cervical vertebra and fifth lumbar spine. * $P < 0.05$, ** $P < 0.01$, *** $P < 0.001$ when compare to FM-sham group. ### $P < 0.01$, #### $P < 0.001$ when compare to M-sham group. Three mice per group were analyzed. All data were presented as the mean \pm standard deviation. HV, Vickers hardness; FM, female; OVX, ovariectomy; M, male; ORX, orchietomy; a.u., arbitrary unit.

femoral bone, the trabecular network in the centrum of vertebrae is a complex inhomogeneous 3D microstructure, this difference may lead to fluctuations in SMI values (42). In another hand, the Tb.Pf evaluates ratio of concave to convex surfaces to reflect the relation of trabecular plates to rods (33), so it's more suitable for analyzing the plate to rod pattern transformation of vertebrae trabecular bone, and predicting the occurrence of OP.

Due to the limitation of the structure of vertebrae, common mechanical test like three-point bending test is not suitable, so we selected micro-indentation to evaluate the biomechanical difference of the cancellous bone in cervical and lumbar spine six-month post-surgery. The HV showed the higher base-line value of cervical vertebrae than that of the lumbar vertebrae in the unoperated animals, which was consistent with their role as load-bearing bones (Figure 5B). In both operated groups, there're much bigger decrease in cervical vertebrae than in lumbar vertebrae. HV reflects the collagen cross-linking and free volume crystallite-

surrounding space, when it's higher means that the microstructure becomes more loosening (43), indicating the bone microstructure disruption and decalcification occurred much more severely. The HV-based elastic modulus is calculated by the linear estimation (44), showing a similar trend as HV.

In this study, we have validated that the cervical vertebrae, compare to lumbar vertebrae, are more sensitive and susceptible, especially in the early stage of sex hormone deprived OP. Although the above conclusions may not be applicable to other types of OP models not involved in this study, such as aging and drug induction, they have certain reference value and provide clues for our future research. In addition, the positive association between cervical vertebrae and OP has also been observed by other clinical researchers who have established scanning and evaluation method by using the dental cone-beam computed tomography systems (CBCT) (45,46). Although these methods are still not mature, they still verified the feasibility of cervical

spine as an assessment site of OP in clinical practice. With maturation of dental CBCT technology, we believed patients may monitor their OP through cervical vertebrae during dental visits, which plays a role in early warning and diagnosis.

Conclusions

In conclusion, cervical vertebrae could be an alternative of traditional lumbar vertebra, together with femur to improve the efficiency and accuracy of OP evaluation, and also be used as a substitute to the femur to provide comparable stage bio-samples like nucleic acids and proteins for analysis in study about early OP animal models.

Acknowledgments

Funding: This work was supported by the National Key Research and Development Program of China (No. 2021YFA0719303), National Natural Science Foundation of China (No. 32100572), Shenzhen Science and Technology Program (Nos. JCYJ20200109115441918, JCYJ20210324102013035 and JCYJ20210324123610028), Shenzhen Key laboratory of Metabolic Health (No. ZDSYS20210427152400001).

Footnote

Reporting Checklist: The authors have completed the ARRIVE reporting checklist. Available at <https://qims.amegroups.com/article/view/10.21037/qims-22-717/rc>

Conflicts of Interest: All authors have completed the ICMJE uniform disclosure form (available at <https://qims.amegroups.com/article/view/10.21037/qims-22-717/coif>). The authors have no conflicts of interest to declare.

Ethical Statement: The authors are accountable for all aspects of the work in ensuring that questions related to the accuracy or integrity of any part of the work are appropriately investigated and resolved. This study was approved by the Ethics Committee for Animal Research, Shenzhen Institutes of Advanced Technology, Chinese Academy of Sciences (No. SIAT-IACUU-201225-YYS-TB-A1640), in compliance with institutional guidelines for the care and use of animals.

Open Access Statement: This is an Open Access article

distributed in accordance with the Creative Commons Attribution-NonCommercial-NoDerivs 4.0 International License (CC BY-NC-ND 4.0), which permits the non-commercial replication and distribution of the article with the strict proviso that no changes or edits are made and the original work is properly cited (including links to both the formal publication through the relevant DOI and the license). See: <https://creativecommons.org/licenses/by-nc-nd/4.0/>.

References

1. Harvey N, Dennison E, Cooper C. Osteoporosis: impact on health and economics. *Nat Rev Rheumatol* 2010;6:99-105.
2. Eastell R, O'Neill TW, Hofbauer LC, Langdahl B, Reid IR, Gold DT, Cummings SR. Postmenopausal osteoporosis. *Nat Rev Dis Primers* 2016;2:16069.
3. Compston JE, McClung MR, Leslie WD. Osteoporosis. *Lancet* 2019;393:364-76.
4. Stavnichuk M, Mikolajewicz N, Corlett T, Morris M, Komarova SV. A systematic review and meta-analysis of bone loss in space travelers. *NPJ Microgravity* 2020;6:13.
5. Sugimoto T, Sato M, Dehle FC, Brnabic AJ, Weston A, Burge R. Lifestyle-Related Metabolic Disorders, Osteoporosis, and Fracture Risk in Asia: A Systematic Review. *Value Health Reg Issues* 2016;9:49-56.
6. Wong SK, Chin KY, Suhaimi FH, Ahmad F, Ima-Nirwana S. The Relationship between Metabolic Syndrome and Osteoporosis: A Review. *Nutrients* 2016.
7. Si L, Winzenberg TM, Jiang Q, Chen M, Palmer AJ. Projection of osteoporosis-related fractures and costs in China: 2010-2050. *Osteoporos Int* 2015;26:1929-37.
8. Komori T. Animal models for osteoporosis. *Eur J Pharmacol* 2015;759:287-94.
9. Watts NB. Postmenopausal Osteoporosis: A Clinical Review. *J Womens Health (Larchmt)* 2018;27:1093-6.
10. D'Amelio P, Isaia GC. Male Osteoporosis in the Elderly. *Int J Endocrinol* 2015;2015:907689. Erratum in: *Int J Endocrinol* 2017;2017:9839017.
11. Tuck SP, Datta HK. Osteoporosis in the aging male: treatment options. *Clin Interv Aging* 2007;2:521-36.
12. Bliuc D, Nguyen ND, Milch VE, Nguyen TV, Eisman JA, Center JR. Mortality risk associated with low-trauma osteoporotic fracture and subsequent fracture in men and women. *JAMA* 2009;301:513-21.
13. Sophocleous A, Idris AI. Rodent models of osteoporosis. *Bonekey Rep* 2014;3:614.

14. Qin L, Yao D, Zheng L, Liu WC, Liu Z, Lei M, et al. Phytomolecule icaritin incorporated PLGA/TCP scaffold for steroid-associated osteonecrosis: Proof-of-concept for prevention of hip joint collapse in bipedal emus and mechanistic study in quadrupedal rabbits. *Biomaterials* 2015;59:125-43.
15. Olson ME, Bruce J. Ovariectomy, ovariectomy and orchidectomy in rodents and rabbits. *Can Vet J* 1986;27:523-7.
16. Jee WS, Yao W. Overview: animal models of osteopenia and osteoporosis. *J Musculoskelet Neuronal Interact* 2001;1:193-207.
17. *The Laboratory Mouse*. Burlington, MA: Academic Press, 2004.
18. Chen H, Kubo KY. Segmental variations in trabecular bone density and microstructure of the spine in senescence-accelerated mouse (SAMP6): a murine model for senile osteoporosis. *Exp Gerontol* 2012;47:317-22.
19. Graf W, de Waele C, Vidal PP. Functional anatomy of the head-neck movement system of quadrupedal and bipedal mammals. *J Anat* 1995;186 (Pt 1):55-74.
20. Charan J, Kantharia ND. How to calculate sample size in animal studies? *J Pharmacol Pharmacother* 2013;4:303-6.
21. Arnold P. Evolution of the Mammalian Neck from Developmental, Morpho-Functional, and Paleontological Perspectives. *Journal of Mammalian Evolution* 2021;28:173-83.
22. Kuo TR, Chen CH. Bone biomarker for the clinical assessment of osteoporosis: recent developments and future perspectives. *Biomark Res* 2017;5:18.
23. Naylor K, Eastell R. Bone turnover markers: use in osteoporosis. *Nat Rev Rheumatol* 2012;8:379-89.
24. Chow DH, Suen PK, Huang L, Cheung WH, Leung KS, Ng C, Shi SQ, Wong MW, Qin L. Extracorporeal shockwave enhanced regeneration of fibrocartilage in a delayed tendon-bone insertion repair model. *J Orthop Res* 2014;32:507-14.
25. Jilka RL, Girasole G, Passeri G, Cooper S, Hangoc G, Abrams J, Broxmeyer H, Manolagas SC. Ovariectomy in the Mouse up-Regulates Hematopoietic Precursors in the Bone-Marrow and Their Progeny in the Peripheral-Blood - a Mediating Role of Il-6. *Journal of Bone and Mineral Research* 1992;7:S115.
26. Jilka RL, Hangoc G, Girasole G, Passeri G, Williams DC, Abrams JS, Boyce B, Broxmeyer H, Manolagas SC. Increased osteoclast development after estrogen loss: mediation by interleukin-6. *Science* 1992;257:88-91.
27. Trajanoska K, Rivadeneira F. The genetic architecture of osteoporosis and fracture risk. *Bone* 2019;126:2-10.
28. Singh M, Nagrath AR, Maini PS. Changes in trabecular pattern of the upper end of the femur as an index of osteoporosis. *J Bone Joint Surg Am* 1970;52:457-67.
29. Rockoff SD. Radiographic trabecular quantitation of human lumbar vertebrae in situ. I. Theory and method for study of osteoporosis. *Invest Radiol* 1967;2:272-89.
30. Kanis JA. Assessment of fracture risk and its application to screening for postmenopausal osteoporosis: synopsis of a WHO report. WHO Study Group. *Osteoporos Int* 1994;4:368-81.
31. Announcing An NIH Consensus Development Conference on Osteoporosis. *Endocrinology* 1984;114:246.
32. Galbusera F, Bassani T. *The Spine: A Strong, Stable, and Flexible Structure with Biomimetics Potential*. Biomimetics (Basel) 2019.
33. Smit TH. The use of a quadruped as an in vivo model for the study of the spine - biomechanical considerations. *Eur Spine J* 2002;11:137-44.
34. Golds G, Houdek D, Arnason T. Male Hypogonadism and Osteoporosis: The Effects, Clinical Consequences, and Treatment of Testosterone Deficiency in Bone Health. *Int J Endocrinol* 2017;2017:4602129.
35. Vanderschueren D, Vandenput L, Boonen S, Lindberg MK, Bouillon R, Ohlsson C. Androgens and bone. *Endocr Rev* 2004;25:389-425.
36. O'Flaherty EJ. Modeling normal aging bone loss, with consideration of bone loss in osteoporosis. *Toxicol Sci* 2000;55:171-88.
37. Hahn M, Vogel M, Pompesius-Kempa M, Delling G. Trabecular bone pattern factor--a new parameter for simple quantification of bone microarchitecture. *Bone* 1992;13:327-30.
38. Hildebrand T, Rüegsegger P. Quantification of Bone Microarchitecture with the Structure Model Index. *Comput Methods Biomech Biomed Engin* 1997;1:15-23.
39. Salmon PL, Ohlsson C, Shefelbine SJ, Doube M. Structure Model Index Does Not Measure Rods and Plates in Trabecular Bone. *Front Endocrinol (Lausanne)* 2015;6:162.
40. Brandi ML. Microarchitecture, the key to bone quality. *Rheumatology (Oxford)* 2009;48 Suppl 4:iv3-8.
41. Kalpakcioglu BB, Morshed S, Engelke K, Genant HK. Advanced imaging of bone macrostructure and microstructure in bone fragility and fracture repair. *J Bone Joint Surg Am* 2008;90 Suppl 1:68-78.
42. Chen H, Zhou X, Fujita H, Onozuka M, Kubo KY. Age-related changes in trabecular and cortical bone

- microstructure. *Int J Endocrinol* 2013;2013:213234.
43. Lees S. A model for bone hardness. *J Biomech* 1981;14:561-7.
 44. Lawn BR, Howes VR. Elastic Recovery at Hardness Indentations. *Journal of Materials Science* 1981;16:2745-52.
 45. Moon ES, Kim S, Kim N, Jang M, Deguchi T, Zheng FY, Lee DJ, Kim DG. Aging Alters Cervical Vertebral Bone Density Distribution: A Cross-Sectional Study. *Applied Sciences-Basel* 2022;12:3143-53.
 46. Slaidina A, Nikitina E, Abeltins A, Soboleva U, Lejniaks A. Gray values of the cervical vertebrae detected by cone beam computed tomography for the identification of osteoporosis and osteopenia in postmenopausal women. *Oral Surg Oral Med Oral Pathol Oral Radiol* 2022;133:100-9.

Cite this article as: Teng B, Yu XF, Li J, Udduttula A, Ismayil A, Huang X, Li J, Zhao PY, Kerem G, Long J, Liu C, Ren PG. Cervical vertebrae for early bone loss evaluation in osteoporosis mouse models. *Quant Imaging Med Surg* 2023;13(4):2466-2477. doi: 10.21037/qims-22-717

Appendix 1 Material and methods

Histologic staining

After the micro-CT analysis, the C5 and L5 samples were dissected and fixed in 4% paraformaldehyde (pH 7.4) for 48 h. Then they were dehydrated in a graded series of ethanol (EtOH) to eliminate the entire water content of these samples: starting from twice in 70% EtOH, twice in 96% EtOH, and twice in 100% ethanol in a vacuum for at least one hour in each step. After the samples were immersed in xylene for one hour, they underwent an infiltration process by placing the samples into a solution of MMA and dibutyl phthalate (6:1) for 24 h, consequently in fresh MMA, dibutyl phthalate (6:1) and 1% benzoyl peroxide solution for 24 h. Embedding of the infiltrated specimens was done in fresh MMA, dibutyl phthalate (6:1), 2.5% benzoyl peroxide solution and 1% polyethylene glycol for 24 h. Polymerization was completed within 3-5 days. However, only three samples from each group were successfully embedded. These samples were sectioned in a mid-sagittal section of thickness 200 μm by using a microtome (EXAKT E300CP, Leica Instruments, Germany), and grinded to a thickness of 150 μm with grinding machine (Mecatech334, Presi, France). One slices from each sample was selected for histologic staining. Stevenel's blue and fuchsin staining allows us to assess the presence of fibrous and bone tissue. The slices (n=3 per group) were stained with Stevenel's blue and fuchsin staining for microscopic identification of the regions of interest (ROIs) under microscope for subsequent micro-indentation testing.

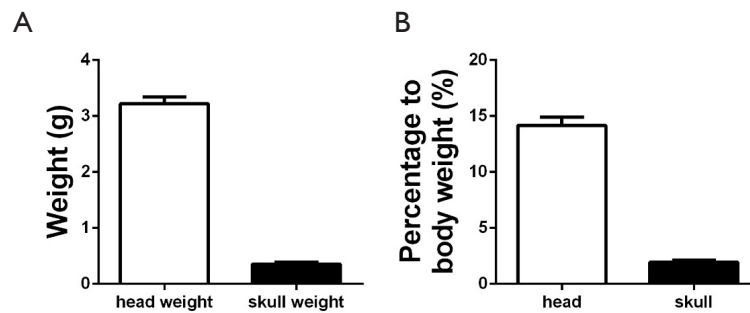


Figure S1 The weight of the head and skull of the mice, and their proportion of the body weight. Five wild type C57BL/6J mice were used, and their weight is about 25 g. (A) Weight of the head and skull of the mouse. (B) The percentage of head and skull to body weight.

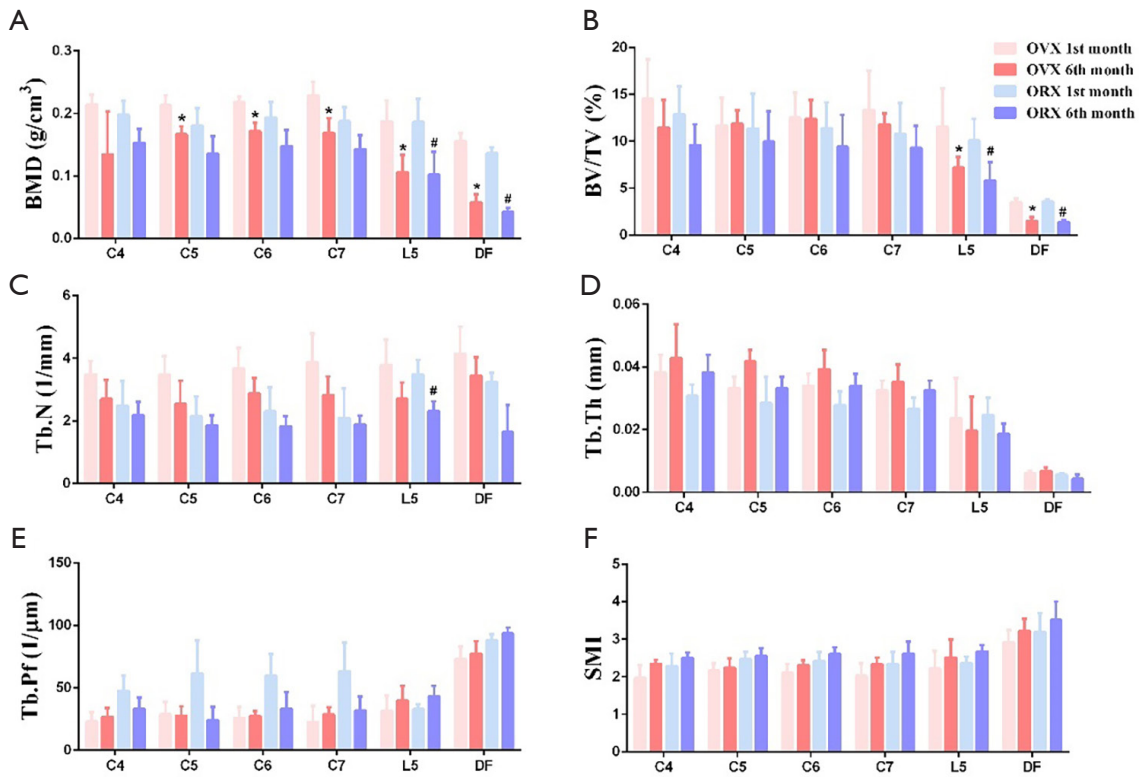


Figure S2 (A) Bone mineral density. (B) Bone volume *vs.* tissue volume. (C) Trabecular thickness. (D) Trabecular number. (E) Trabecular pattern factor. (F) Structure model index. * $P < 0.05$ when compare to OVX first month group. # $P < 0.05$ when compare to ORX first month group. Five mice per group were analyzed.

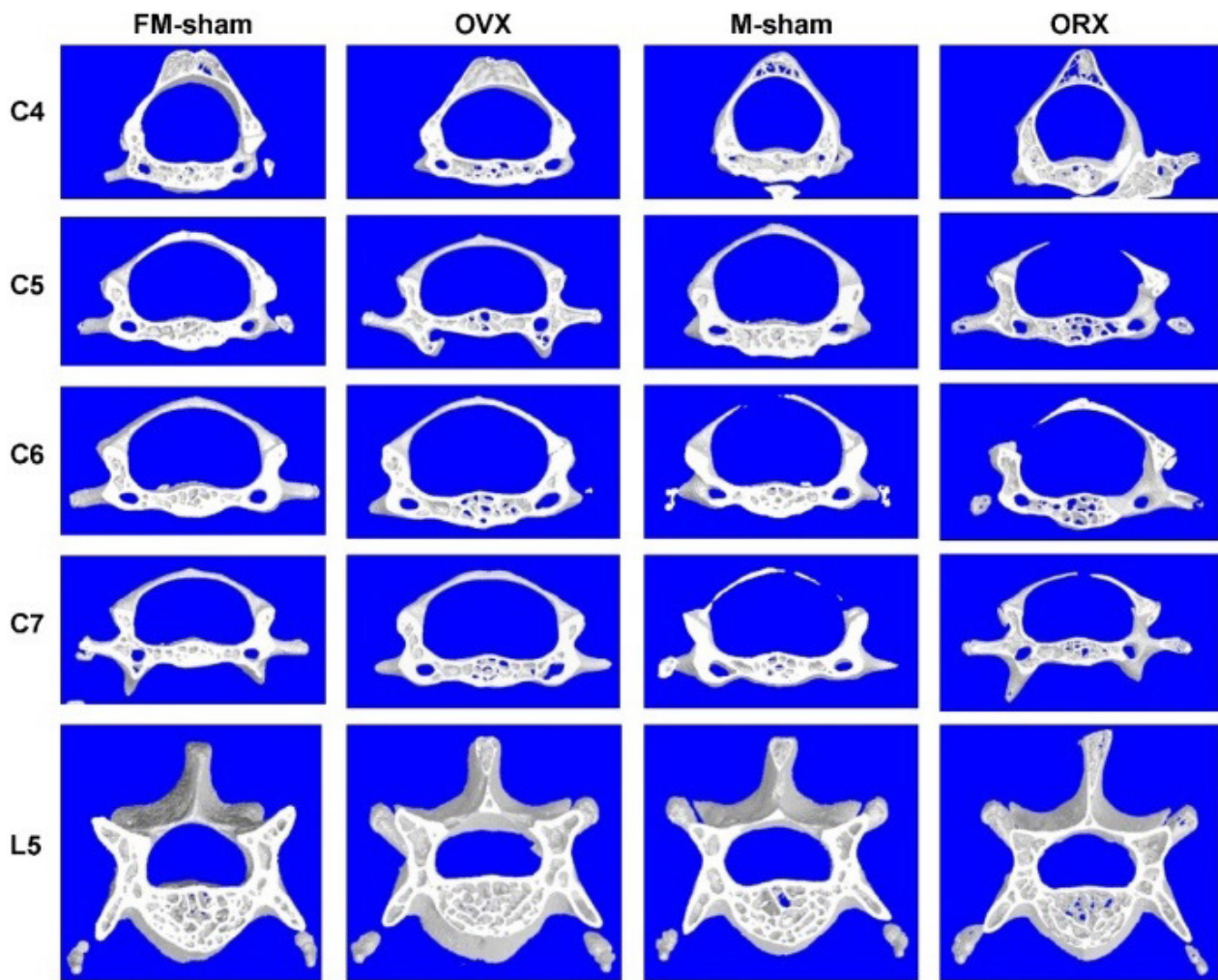


Figure S3 The exemplary 3D image from the micro-CT analysis of the different cervical vertebra and fifth lumbar from different group at first month. The female sham mice group, OVX mice group, male sham mice group and ORX mice group were shown from left to right in each column of the figure.

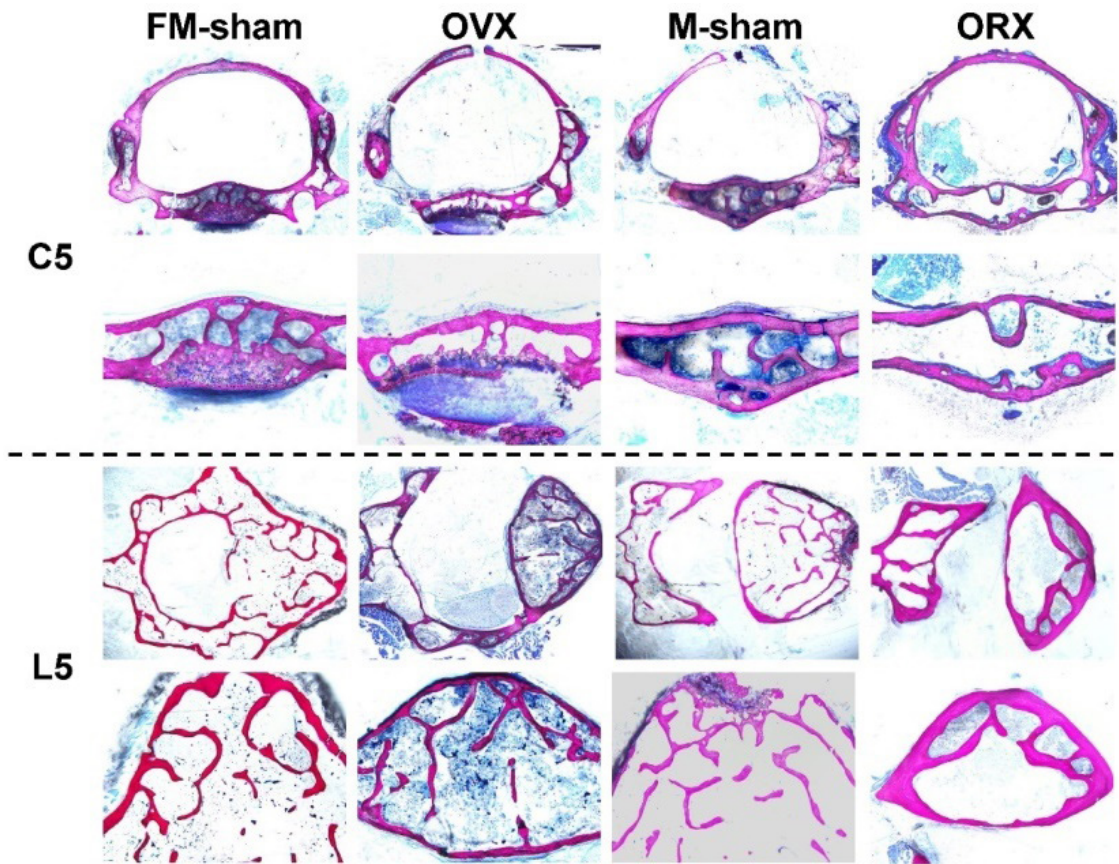


Figure S4 Stevenel's blue and fuchsin staining of the fifth cervical vertebra and fifth lumbar from different group six-month post-gonadectomy. The tissue stained with blue was the muscle and fibrocartilage. The tissue stained with red was the bone. The female sham mice group, OVX mice group, male sham mice group and ORX mice group were shown from left to right in each column of the figure.